Simulation of nonlinear wave elevation around a square array of truncated cylinders

B. Teng and P. W. Cong
State Key Laboratory of Coastal and Offshore Engineering
Dalian University of Technology
Dalian 116024, Liaoning, China
E-mail: bteng@dlut.edu.cn

1. INTRODUCTION

An arrangement of four truncated cylinders centered at the corners of a square is a simple model of a typical TLP platform. The prediction of wave run-up around the cylinders is of great interest for the offshore industry, e.g. to determine the height of the platform deck above the sea level. Computations indicate that resonant wave motion may occur inside the four-cylinder structure, which can lead to large wave height between structures, and also to enhanced wave forces on individual columns. If these large wave loads and free-surface elevations occur in practice, it would have serious implications for the design of large arrays of offshore structures. It is therefore important to understand when these effects occur, and how they might be affected by factors, such as structure form and nonlinearity.

Although some interesting interaction effects that arise from nonlinearity have been observed, nonlinear effects are difficult to analyze for complex geometries. The nonlinear wave diffraction by a square array of truncated cylinders has received relatively less attention. In present study, the interaction between a square array of truncated cylinders is investigated in frequency domain, based on a Stokes expansion approach. The solution for the second-order potential is obtained by a boundary-integral equation method. Numerical calculation is performed for the wave run-up and free-surface elevation to the second order accuracy. Numerical results show that the near-trapping phenomena occurs inside the four-cylinder structure, which leads to large wave height. The second order contributions to the free surface elevation can be considerable especially at critical frequencies.

2. MATHEMATICAL FORMULATION AND METHODS

We consider the case when a fixed body is placed in an incoming wave system with angular frequencies ω, amplitude A and in a water of depth d. The coordinate system has the z-axis pointing vertically upwards and origin is at the undisturbed free surface. The incident wave makes an angle β with the positive x-axis. We adopt the usual framework of potential flow theory, assuming that the fluid is incompressible and irrotational, so that the governing equation in the fluid becomes Laplace's equation for the velocity potential. The total velocity potential can be expanded in a perturbation series in terms of the wave slope parameter ε.

Here we are interested only in the periodic components. At each order, we depose ϕ into incident (ϕ_I) and diffracted (ϕ_D) potentials: $\phi^{(i)}=\phi_I^{(i)}+\phi_D^{(i)}$, i=1,2. The incidence potentials are given from Stokes's waves. After introducing the perturbation series into the original nonlinear boundary value problem (BVP), we can obtain corresponding BVPs for the potentials at different orders. The second-order problem is complicated by the inhomogeneous forcing term in the free-surface boundary condition, which is given in terms of quadratic products of the first-order potential:

$$Q=\left[-\frac{i\omega}{2g}\phi^{(1)}\left(-\omega^2\frac{\partial\phi^{(1)}}{\partial z}+g\frac{\partial^2\phi^{(1)}}{\partial z^2}\right)+i\omega\left(\nabla\phi^{(1)}\right)^2\right]_{z=0}-Q_I \quad (1)$$

where Q_I represents the contribution from quadratic products of the first-order incident potential itself and it is subtracted out owing to the free-surface condition satisfied by the second-order incident potential. $\nu=\omega^2/g$ is the infinite-depth wave number and g is gravity.

The first-order and the second-order boundary value problems can be solved by boundary integral equation formulated by applying Green's theorem to the fluid domain. The solutions of the first-order diffraction problems are classical and relatively easy to obtain. The second-order diffraction problem is significantly more difficult to implement. Introducing Green function G corresponding to an oscillating source at the frequency 2ω, and applying Green's theorem to $\phi_D^{(2)}$ and G, we can obtain a Fedholm integral equation of the second kind for $\phi_D^{(2)}$ (Eatock Taylor and Chau, 1992)

$$C(\mathbf{x_0})\phi_D^{(2)}(\mathbf{x_0}) - \iint_{S_B} \phi_D^{(2)}(\mathbf{x}) \frac{\partial G(\mathbf{x},\mathbf{x_0})}{\partial n} ds$$

$$= \iint_{S_B} G(\mathbf{x},\mathbf{x_0}) \frac{\partial \phi_I^{(2)}(\mathbf{x})}{\partial n} ds - \iint_{S_F} G(\mathbf{x},\mathbf{x_0}) Q(\mathbf{x}) ds. \quad (2)$$

The coefficient $C(\mathbf{x}_0)$ can lead to difficulties in solving above equation and the integrand has a singularity near to the source point. This can be overcome by Teng and Eatock Taylor's (1995) method.

After solving for the first- and second-order potentials, the associated forces and moments as well as local pressure and wave elevations can be obtained directly. We expand the free-surface elevation also in perturbation series in ε. The expression for the wave elevation is written as follows:

$$\zeta = \zeta^{(1)} + \zeta^{(2)} = \mathrm{Re}\left[\eta^{(1)} e^{-i\omega t} + \eta^{(2)} e^{-2i\omega t} + \overline{\eta}^{(2)}\right]. \quad (3)$$

As velocity potential, the wave elevation can be decomposed into a time-independent term and a double-frequency term, which in turn can be written as a sum of the contributions from the first-order potential ($\eta_q^{(2)}$) and the second-order potential ($\eta_p^{(2)}$)

$$\zeta^{(2)} = \left(\eta_p^{(2)} + \eta_q^{(2)}\right) e^{-2i\omega t} + \overline{\eta}^{(2)}, \quad (4)$$

Each component in Eq. 4 is defined as

$$\eta_p^{(2)} = \frac{2i\omega}{g}\left[\phi_I^{(2)} + \phi_D^{(2)}\right]_{z=0}, \quad (5)$$

$$\eta_q^{(2)} = \left[-\frac{1}{4g}\left(\nabla\phi^{(1)}\right)^2 - \frac{\omega^2}{2g^2}\phi^{(1)}\frac{\partial\phi^{(1)}}{\partial z}\right]_{z=0}, \quad (6)$$

$$\overline{\eta}^{(2)} = \left[-\frac{1}{4g}\left|\nabla\phi^{(1)}\right|^2 + \frac{\omega^2}{2g^2}\phi^{(1)}\frac{\partial\phi^{(1)*}}{\partial z}\right]_{z=0}. \quad (7)$$

3. CONVERGENCE TEST

The convergence of the present solution will be examined in this section. The test case considered is four vertical cylinders with radius a centered at the corners of a square with side length $4a$. The centers of the cylinders are located at ($\pm 2a$, $\pm 2a$), and the cylinders are numbered anti-clockwise with cylinder number 1 located in the first quadrant. A local coordinate system is located at each cylinder with the origin at the centre of the cylinder and the local axes are parallel to the axes in the global coordinate system. Fig. 1 shows the definition of the global and the local coordinate systems. In the test cases the direction of the incident wave is 45 degrees with respect to the x direction and the water depth $h=3a$.

Only a quarter area is discretized by using simplification on its geometry symmetry. The first region S_1 on the free surface is meshed in a round form with an outer radius b and totally N_F quadrilateral elements are employed. In the outermost region S_3, Hankel's asymptotic expansions are substituted into the integrand. The regions S_2 and S_3 do not need to be discretized. The cylinders are discretized with N_B quadrilateral elements. There are n_z panels in the vertical direction and n_c panels in the circumferential direction.

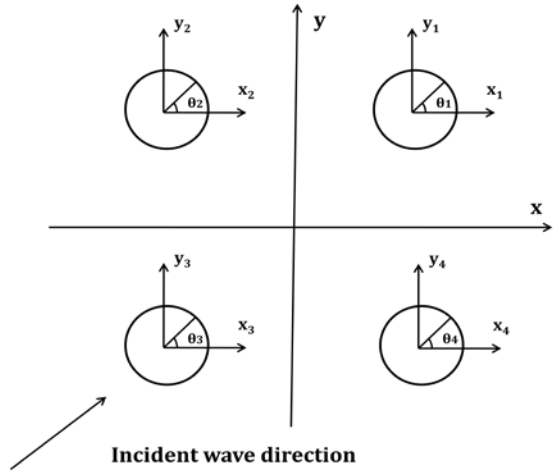

Fig. 1 Definition of global and local coordinate systems

For this configuration we have chosen ka =1.1, where k is the linear wave number. The different parameters that describe the discretization are listed in Table 1. From Fig. 2 we see that the two test cases give almost the same results even though the discretization in case 2 is much coarser than the discretization in case 1. We conclude that convergence is achieved. The curves obtained by the present results and Malenica et al's (1999) results are in good agreement which confirm that convergence has been achieved.

Table 1 Parameters associated with the discretization of the body and the free surface.

Case	Body surface			Free surface	
	n_z	n_C	N_B	N_F	b
1	25	64	1600	5647	12a
2	24	48	1152	3027	10a

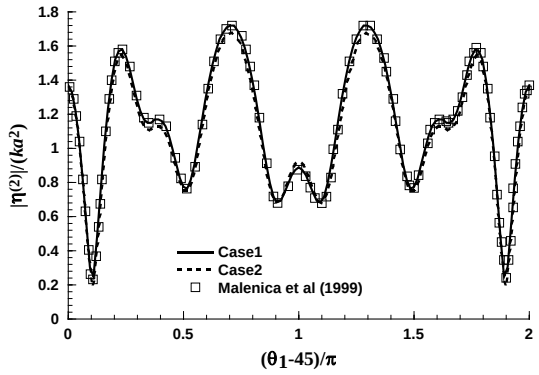

Fig. 2 The total second-order wave run-up amplitude around the cylinder 1

4. NUMERICAL RESULTS AND DISCUSSION

In this section we give the results for second-order quantities for the square array of truncated cylinders. In this case, n_c=48, n_z=24, and n_r (the number of panels in the radial direction) =8

are used to mesh the body surface. 3027 quadrilateral elements are used to mesh S_1 and the outer radius b of the first region on the free surface is equal to 10a. The mesh on the body surface and free surface are shown in Fig. 3.

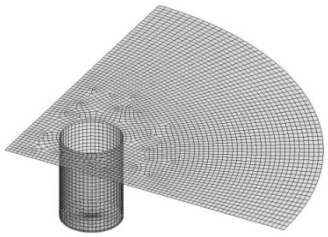

Fig. 3 The body surface and free surface mesh of the structure without pontoons

With application the direct method for the second problems, the second order potential is computed, and furthermore the second order kinematics, like second order wave elevation can be computed. Figs. 4~7 show the max free-surface elevations at the following five points: T_1=(2.707a, 2.707a), T_2=(1.293a, 1.293a), T_3=(0.0, 0.0), T_4=(-1.293a, -1.293a), and T_5=(-2.707a, -2.707a) for the non-dimensional frequency ka from 0.1~1.8 and the non-dimensional incident wave amplitude kA=0.2. One can observe that the max free-surface elevation predicted by the linear wave theory is significantly increased especially at T_2 when ka is near 1.68. The individual second-order components $|\eta_q^{(2)}|$ and $|\eta_p^{(2)}|$ are also large when ka is near 1.68 but due to their phase differences the associated total harmonic second-order elevation is small. At the same time, the second-order time-independent component that can be computed directly from the first order potential for monochromatic incident waves has a considerable effect on the total wave field and so should not be neglected during design. When ka is near 0.42, the linear elevation at these points is seen to be small, whereas the elevation predicted by the second-order wave theory is now large especially in Figs. 5~6. It is clear that the above-mentioned large increases in wave elevation only occur over a very narrow range of frequencies, close to what we might now describe as the near-trapping. This highly significant result suggests that near-trapping of the second-order wave occurs when its frequency coincides with the linear near-trapping frequency as found by Malenica et al. (1999). If ka apart from near-trapping frequency, large magnification effects would not be anticipated.

Figs. 9~11 show the variation of the maximum wave run-up around the cylinders with the non-dimensional frequency ka=0.42 and the non-dimensional incident wave amplitude kA=0.2. The results predicted by both linear wave theory and the second-order wave theory are shown. These figures illustrate that the effect of the second-order nonlinearity on the wave run-up becomes very significant at this frequency. At the same location, the linear wave theory largely under-predicts the wave height. The second order harmonic component's contribution to the free surface elevation plays a strong role. The second order diffraction should be included into the design process for air gap rather than ignored.

All these above results confirm the importance of the influence of interaction between cylinders on the final results.

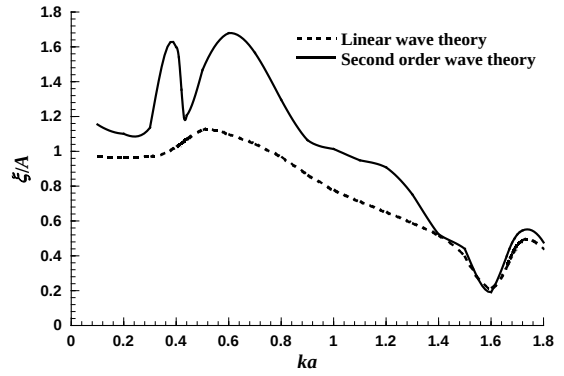

Fig 4. The max free-surface elevation at T_1.

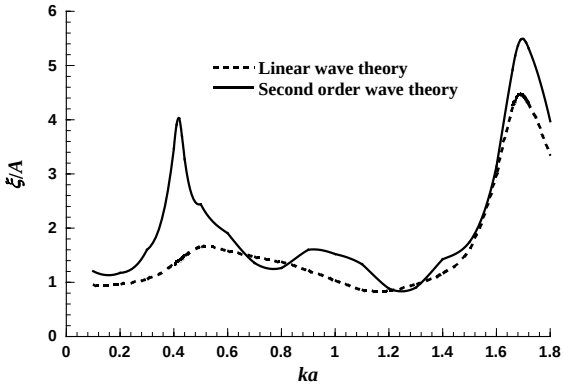

Fig 5. The max free-surface elevation at T_2.

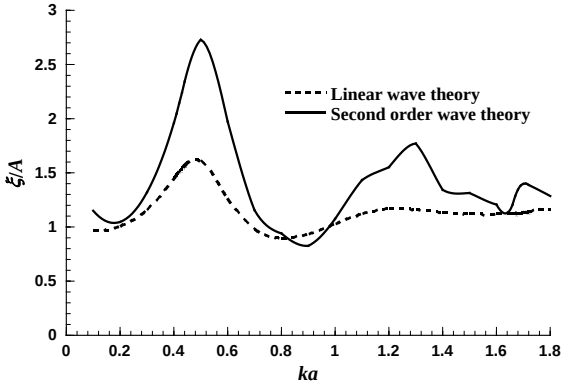

Fig 6. The max free-surface elevation at T_3.

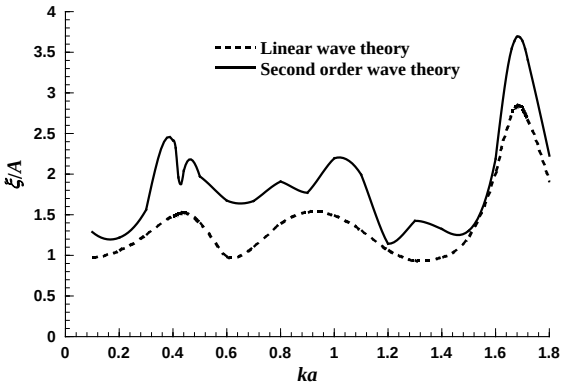

Fig. 7 The max free-surface elevation at T_4.

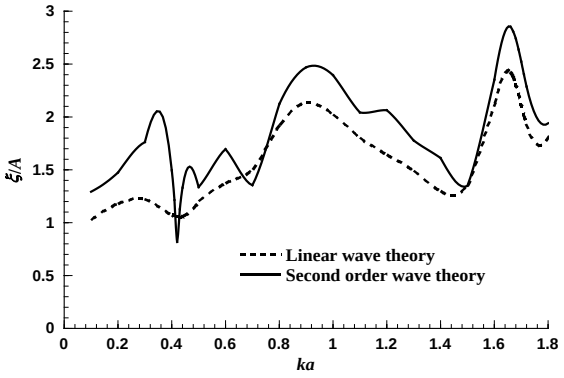

Fig. 8 The max free-surface elevation at T_5.

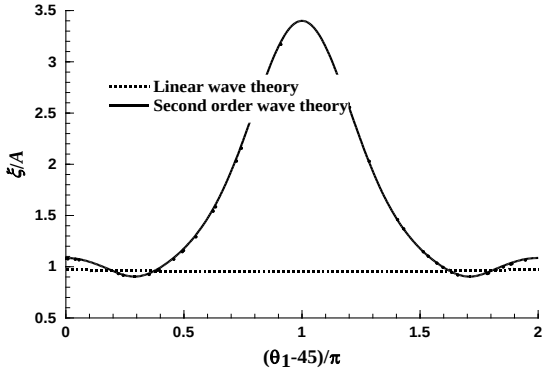

Fig. 9 Max wave run-up around cylinder 1

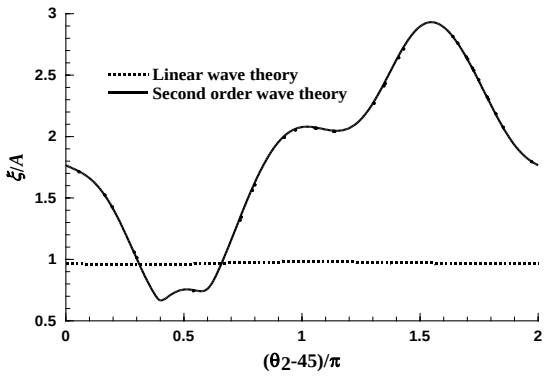

Fig. 10 Max wave run-up around cylinder 2

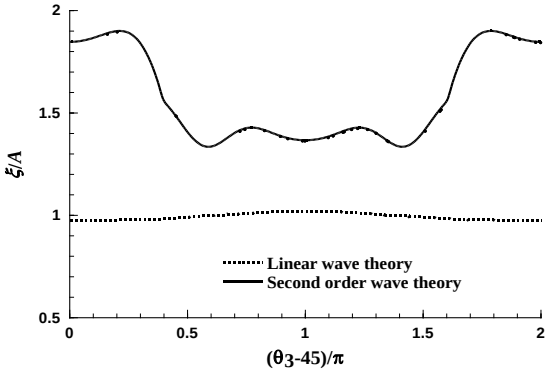

Fig. 11 Max wave run-up around cylinder 3

5. Conclusion

Nonlinear diffraction of regular waves by a square array of truncated cylinders is investigated in frequency domain. Numerical calculation is performed for the wave run-ups and free-surface elevation by both linear wave theory and the second-order wave theory. All the results confirm the importance of the influence of interaction between cylinders. Near-trapping is shown to play a strong role, not only for the first-order solution but also for the second-order solution when the second-harmonic of the wave frequency coincides with the frequency of the trapped mode. The second order contributions to the free surface elevation can be considerable especially at critical frequencies. The second order diffraction should be included into the design process for air gap rather than ignored.

6. References

[1]. Birknes, J., 2001, A convergence study of second-order wave elevation on four cylinders. Proceedings of the 11th ISOPE conference, Stavanger, Norway, vol. III, pp. 392–399.

[2]. Eatock Taylor, R., and Chau, F.P., 1992, Wave diffraction theory — some developments in linear and nonlinear theory, J Offshore Mech and Arctic Eng, 114, 185-194.

[3]. Malenica, S., Eatock Taylor, R. and Huang J.B., 1999, Second-order wave diffraction by an array of vertical cylinders. J Fluid Mech, 390:349~373.

[4]. Teng, B. and Eatock Taylor, R., 1995, New higher-order boundary element methods for wave diffraction/radiation. Applied Ocean Research. 17(2): 71-77.